

Morphologic and Molecular Features of Hepatocellular Adenoma with Gadoteric Acid–enhanced MR Imaging¹

Ahmed Ba-Ssalamah, MD
 Céilia Antunes, MD
 Diana Feier, PhD, MD²
 Nina Bastati, MD
 Jacqueline C. Hodge, MD
 Judith Stift, MD
 Maria A. Cipriano, MD
 Friedrich Wrba, MD
 Michael Trauner, MD
 Christian J. Herold, MD
 Filipe Caseiro-Alves, MD

Purpose:

To evaluate the diagnostic performance of imaging features of gadoteric acid–enhanced magnetic resonance (MR) imaging to differentiate among hepatocellular adenoma (HCA) subtypes by using the histopathologic results of the new immunophenotype and genotype classification and to correlate the enhancement pattern on the hepatobiliary phase (HBP) with the degrees of expression of organic anion transporting polypeptide (OATP1B1/3), multidrug resistance-associated protein 2 (MRP) (MRP2), and MRP 3 (MRP3) transporters.

Materials and Methods:

This retrospective study was approved by the institutional review board, and the requirement for informed consent waived. MR imaging findings of 29 patients with 43 HCAs were assessed by two radiologists independently then compared with the histopathologic analysis as the standard of reference. Receiver operating characteristic curves and Spearman rank correlation coefficient were used to test the diagnostic performance of gadoteric acid–enhanced MR imaging features, which included the retention or washout at HBP and degree of transporter expression. Interreader agreement was assessed by using the κ statistic with 95% confidence interval.

Results:

The area under the curve for the diagnosis of inflammatory HCA was 0.79 (95% confidence interval: 0.64, 0.90); for the steatotic type, it was 0.90 (95% confidence interval: 0.77, 0.97); and for the β -catenin type, it was 0.87 (95% confidence interval: 0.74, 0.95). There were no imaging features that showed a significant statistical correlation for the diagnosis of unclassified HCAs. On immunohistochemical staining, OATP1B1/3 expression was the main determinant for the retention, whereas MRP3 was the key determinant for washout of gadoteric acid at HBP ($P < .001$). MRP2 appeared to have no role.

Conclusion:

Gadoteric acid–enhanced MR imaging features may suggest the subtype of HCA. The degree of OATP1B1/3 and MRP3 expression correlated statistically with gadoteric acid retention and washout, respectively, in the HBP.

©RSNA, 2015

Online supplemental material is available for this article.

¹From the Department of Biomedical Imaging and Image-guided Therapy (A.B.S., D.F., N.B., J.C.H., C.J.H.), Department of Pathology (J.S., F.W.), and Division of Gastroenterology and Hepatology, Department of Internal Medicine III (M.T.), Medical University of Vienna, Waehringer Guertel 18-20, A-1090 Vienna, Austria; and Clínica Universitária de Radiologia, Faculty of Medicine (C.A., F.C.A.), and Serviço de Anatomia Patológica (M.A.C.), University Hospital of Coimbra, Coimbra, Portugal. Received October 7, 2014; revision requested November 17; revision received January 28, 2015; accepted February 19; final version accepted March 12. **Address correspondence to** N.B. (e-mail: nina.bastati@meduniwien.ac.at).

²**Current address:** Department of Imaging, Iuliu Hatieganu University of Medicine and Pharmacy, Cluj-Napoca, Romania.

©RSNA, 2015

Hepatocellular adenoma (HCA) poses a diagnostic challenge because its imaging appearance and enhancement patterns at cross-sectional imaging, including computed tomographic (CT) and magnetic resonance (MR) imaging, are variable (1–4). The histopathologic work-up may be an equal challenge (5,6). Recently, HCA was subdivided into four types according to the Bordeaux group by using genotype and phenotype classification (7–9). Because HCAs have diverse clinical courses on the basis of their subtype, medical versus surgical management may rely on an accurate imaging classification (10). The value of MR

imaging to distinguish between these subgroups was described in some recent publications on the basis of specific features and contrast agent–enhancement pattern (1,4,11,12). In particular, in the hepatobiliary phase (HBP) of MR imaging after administration of the contrast agent (ie, 20 minutes after the administration of gadoteric acid [Primovist or Eovist; Bayer Healthcare, Berlin, Germany]), the majority of HCAs show washout and appear hypointense to the surrounding liver tissue (13,14). Increasingly, the literature (15–18) contains reports of HCA nodules that show incomplete washout or even retention of gadoteric acid during the HBP. Some theories suggest that these different enhancement patterns could be related to the subtype of the adenoma and subsequently the amount and location of different transporter proteins, such as organic anion transporting polypeptide (OATP) 1B1/3 (OATP1B1/3) and multidrug resistance–associated protein 2 (MRP) (MRP 2) and 3 (MRP3), which mediate the uptake and canalicular or basolateral excretion of gadoteric acid during the HBP, respectively (19,20).

The expression of these transporters and their role in contrast-material uptake after the injection of gadoteric acid underwent pathologic and radiologic study, but only in HCCs within the context of liver cirrhosis (21–23). To our knowledge, the role

of the three key hepatobiliary transporters was not systematically studied in patients with HCAs.

The purpose of our study was twofold: to evaluate the diagnostic performance of imaging features of gadoteric acid–enhanced MR imaging to distinguish between the four HCA subtypes by using the histopathologic results according to the new immunophenotype and genotype classification, described by the Bordeaux group (7,10), as the standard of reference, and to correlate the retention or washout on the HBP phase with the degree of expression of OATP1B1/3, MRP2, and MRP3 transporters (24).

Advances in Knowledge

- We found a statistically significant difference in the enhancement pattern of gadoteric acid among the four subtypes of hepatocellular adenomas (HCAs) ($P = .001$); at the hepatobiliary phase (HBP), all steatotic and unclassified HCAs showed washout of contrast media, while six of 21 (39%) inflammatory and five of six (83%) of β -catenin HCAs retained contrast media at 20 minutes.
- All tumors that showed equivocal or increased expression of organic anion transporting polypeptide (OATP) (OATP1B1/3) showed gadoteric acid retention on HBP images (11 of 11 [100%]), while tumors that showed decreased or no expression of OATP1B1/3 tended to show contrast agent washout on HBP images (21 of 32 [66%]) ($P < .001$).
- All tumors that showed decreased or no expression of multidrug resistance–associated protein 3 (MRP) (MRP3) showed contrast-media retention on HBP images (11 of 11 [100%]), while tumors that showed equivalent or increased expression of MRP3 tended to show gadoteric acid washout on HBP images (15 of 32 [47%]) ($P = .008$).

Implication for Patient Care



- Noninvasive gadoteric acid–enhanced MR classification of HCA subgroups on the basis of the morphologic features and enhancement pattern is important because it substantially influences management: for steatotic, unclassified, and inflammatory HCAs that do not exceed 5 cm in diameter or that do not grow, follow-up is sufficient; however, surgical resection is indicated if any of these lesions markedly increases in size, and surgical resection is the treatment of choice for any β -catenin HCA, independent of size.

Materials and Methods

Patients

Retrospective data collection and analysis were approved by the ethics review boards of the two participating hospitals; the requirement for informed consent was waived. We enrolled 29 patients with 43 HCA lesions. These patients came from the institutional databases between 2007 and 2013. We included only those patients who underwent gadoteric acid–enhanced

Published online before print

10.1148/radiol.2015142366 Content codes:  

Radiology 2015; 000:1–10

Abbreviations:

HBP = hepatobiliary phase
HCA = hepatocellular adenoma
MRP = multidrug resistance–associated protein
OATP = organic anion transporting polypeptide
PV = portal venous

Author contributions:

Guarantors of integrity of entire study, A.B.S., N.B., F.W., C.J.H.; study concepts/study design or data acquisition or data analysis/interpretation, all authors; manuscript drafting or manuscript revision for important intellectual content, all authors; approval of final version of submitted manuscript, all authors; agrees to ensure any questions related to the work are appropriately resolved, all authors; literature research, A.B.S., C.A., N.B., J.C.H., J.S., F.W., M.T., C.J.H., F.C.A.; clinical studies, A.B.S., C.A., N.B., M.A.C., M.T.; experimental studies, M.T.; statistical analysis, A.B.S., D.F., J.C.H.; and manuscript editing, A.B.S., D.F., N.B., J.C.H., F.W., M.T., C.J.H., F.C.A.

Conflicts of interest are listed at the end of this article.

Figure 1

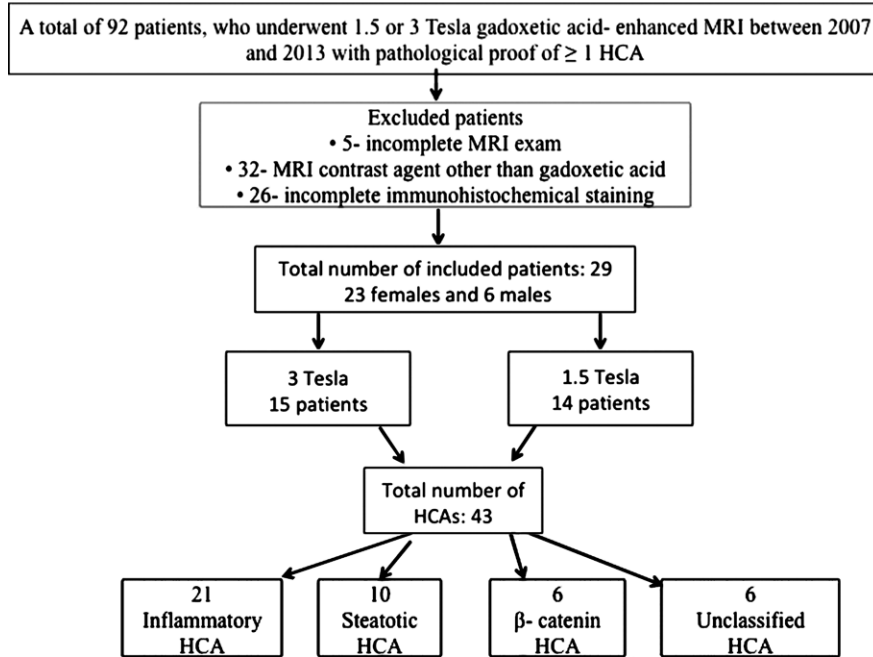


Figure 1: Flowchart shows the excluded and included patients.

MR imaging and in whom we obtained pathologic proof of the diagnosis in one or more lesions, either after surgery (21 patients with 35 lesions) or after CT- or ultrasonographically guided biopsy (eight patients with eight lesions). A study coordinator (D.F., a radiologist with 6 years of experience) was aware of which nodule or nodules underwent pathologic verification with MR images of patients with multiple HCAs. The MR findings of these nodules were independently evaluated by two radiologists and subsequently compared with the histologic results. The mean time interval between the gadoteric acid-enhanced MR examination and surgery or biopsy of the lesion was 119.8 days \pm 4.3 (standard deviation) (range, 1 day to 4 months). Figure 1 is a flowchart of the excluded and included patients.

MR Examination Protocol

At both institutions, all MR examinations were performed by using either a 3-T or 1.5-T imager (Magnetom Trio Tim or Magnetom Symphony Maestro Class; Siemens Healthcare, Erlangen, Germany) with the following sequences:

T1-weighted in phase and opposed phase, respiratory-triggered T2-weighted fat-suppressed turbo spin echo, and three-dimensional fat-suppressed gradient-echo T1-weighted acquisitions. Dynamic gadoteric acid-enhanced sequences were performed by using a bolus tracking system during the arterial phase. The dose of contrast media was based on the weight of the patient (0.025 mmol/kg or 0.1 mL/kg, maximum of 10 mL) and was administered with a power injector (Medrad Spectris Solaris EP MR Injection System; Bayer Healthcare). The flow rate was 1 mL/sec, followed by a 200-mL saline solution flush (administered at 1 mL/sec). The portal venous (PV) and delayed phase images were then acquired at 70 and 300 seconds, respectively. The HBP images were obtained 20 minutes after intravenous administration of gadoteric acid. Table 1 provides the examination parameters.

Image Evaluation

All MR images were retrospectively and independently reviewed on a commercial picture archiving and communication system station (PACS version 5.2;

Agfa Health Care, Mortsel, Belgium) by two observers: a radiologist who specialized in abdominal MR imaging with more than 20 years of experience (A.B.) and a radiologist in her 5th year of training (N.B.). Both radiologists were blinded to the pathologic diagnosis and clinical data. Before interpreting the images, both radiologists met to set the criteria for the interpretation of all sequences of MR examinations. For training purposes, the two readers jointly reviewed 20 sample cases of pathologic analysis-confirmed HCAs, which were not included in this study. They decided to analyze the following: (a) the number of lesions; (b) the diameter of the lesion or lesions; (c) the location of the resected or biopsied lesions on the basis of the Couinaud numbering system; (d) the contour of the nodules (ie, smooth or lobulated); (e) the signal intensity of the lesions on T1- and T2-weighted sequences compared with that of the surrounding liver parenchyma scored as hypointense, isointense, moderately hyperintense, or markedly hyperintense (on T2-weighted images, the signal intensity was considered markedly hyperintense if it was greater than or equal to spleen signal intensity); (f) the appearance of the lesion on each sequence (ie, homogeneous or heterogeneous); (g) the presence of macroscopic hemorrhage, defined as focal T1- and T2-weighted hyperintense and hypointense area, respectively; (h) the presence of a necrotic or cystic component, defined as nonlinear high signal intensity on T2-weighted images, nonenhancing after contrast agent administration, and margins that are not sharp; (i) the presence of a central scar, defined as linear high- or low-signal-intensity area on T2-weighted images, enhancing after contrast agent administration in arterial and PV phases, and washout in the HBP; (j) the presence of a pseudocapsule from compression of normal adjacent liver parenchyma, which was defined as a rim of high signal intensity on T2-weighted images that enhances and retains contrast agent in all phases, including the HBP (if due to vaguely enlarged veins, it appears as a thin hypointense rim at the HBP);

Table 1

Imaging Parameters for 1.5-T and 3-T Imagers

Sequence	Section Thickness (mm)		Intersection Gap		Matrix		TR (msec)		TE (msec)		FOV (mm)	
	1.5 T	3 T	1.5 T	3 T	1.5 T	3 T	1.5 T	3 T	1.5 T	3 T	1.5 T	3 T
In-phase T1-weighted GRE FLASH 2D	6	5	2	1	256 × 192	320 × 240	100	130	2.27	2.46	380	350
Opposed-phase T1-weighted 2D GRE FLASH	6	5	2	1	256 × 192	320 × 240	100	131	5.19	3.69	380	350
Axial precontrast T1-weighted 3D GRE VIBE SPAIR	3–4	1.7	2		256 × 179	256 × 146	4.8	2.67	2.38	0.97	380	430
Axial postcontrast T1-weighted 3D GRE VIBE SPAIR*	3–4	1.7	2		256 × 179	256 × 146	4.8	2.67	2.38	0.97	380	430
Axial T2-weighted fat-suppressed TSE	6	5	2	1	320 × 224	320 × 202	1550	2000	93	95	380	370
HBP axial postcontrast T1-weighted 3D GRE VIBE SPAIR	3–4	1.7	2		256 × 179	256 × 146	4.8	2.67	2.38	0.97	380	430

Note.—2D = Two-dimensional, 3D = three-dimensional, FLASH = fast low angle shot, FOV = field of view, GRE = gradient echo, SPAIR = spectral attenuated inversion recovery, TE = echo time, TR = repetition time, TSE = turbo spin echo, VIBE = volumetric interpolated breath-hold examination.

* Sequence was performed three times: arterial, PV, and delayed.

(k) the presence of fat deposits in the lesion, defined as signal drop on opposed-phase T1-weighted MR images (absence, focal, or diffuse; mild or severe); (l) the presence of steatosis in the nontumoral liver (mild, moderate or severe); (m) enhancement pattern in the arterial, PV, or delayed phase (homogeneous or heterogeneous), and (n) the intensity of enhancement (none; mild, less than PV; moderate, approximately equal to PV; or marked approximately equal to aorta). Furthermore, contrast agent retention or washout in the PV, delayed phases, and HBP was documented.

Finally, from the MR imaging findings evaluated, each radiologist was asked to make an a priori diagnosis for each lesion detected on the basis of typical features of those lesions, as previously published (2,4,11,13–17,25).

An inflammatory HCA was diagnosed if the lesion was moderately to markedly hyperintense at T2, with or without peripheral hyperintensity (pseudocapsule or atoll sign), and hypointense at T1 without signal drop at chemical shift imaging, associated with intense arterial enhancement that persisted in venous and delayed phases,

and presence of steatosis in the nontumoral liver. A lesion with a thick hyperintense rim on T2-weighted images that showed enhancement in arterial and PV phases only, with washout on the HBP, was labeled as the atoll sign, rather than pseudocapsule. Otherwise, it was defined as having a pseudocapsule if it met the criteria defined above.

A steatotic HCA was diagnosed if the lesion showed signal loss at T1 out-of-phase sequences compared with in-phase sequences, moderate arterial enhancement that did not persist into the venous and delayed phases, and moderately high T2 signal intensity.

A β -catenin HCA was diagnosed if the lesion was mainly heterogeneously hyper- and hypointense, respectively, on T2- and T1-weighted precontrast sequences, had a central scar, and had no signal loss at chemical shift imaging. On contrast-enhanced images, the lesion had to be (homogeneously or heterogeneously) hypovascular in the arterial phase and show either persistence (signal intensity unchanged or decreased but still present in the PV phase). In the delayed phase and HBP, lesion conspicuity was compared with that of the surrounding liver parenchyma (ie, relative washout) (18,26).

To our knowledge, no characteristic MR imaging features have yet been proposed for unclassified HCAs (3,4). Therefore, all other HCAs without steatosis and that did not fit the criteria for any other focal liver lesion were assigned unclassified.

Lastly, for each lesion, the retention or washout of gadoteric acid in the HBP was compared with OATP and MRP expression. Finally, lesion features, enhancement patterns, and a priori diagnosis from both readers were compared with the final histopathologic diagnosis. The interreader agreement was calculated.

Histopathologic Analysis and Immunohistochemical Staining

To confirm the diagnosis, all HCA specimens were reviewed again by two liver pathologists (J.S. and F.W., with 7 and 20 years of experience, respectively) in consensus. The final histologic diagnosis of HCA was made according to the accepted criteria (6,8,27). To subtype the HCAs, immunohistochemical stains were applied to paraffin sections including polyclonal antibody liver-fatty acid binding protein (1:100 dilution; Biotechnology, Santa Cruz, Calif),

monoclonal antibody amyloid A (1:800 dilution; Dako, Glostrup, Denmark), monoclonal antibody HSP70 (1:50 dilution; Biotechnology), glutamine synthetase (1:100 dilution, Biocare Medical, Concord, Calif), and monoclonal antibody β -catenin (1:100 dilution; BD Biosciences, San Jose, Calif) (23,24). The primary antibodies used (OATP1B1/3, MRP2, and MRP3) are listed in Table E1 (online) (28,29). HCAs were subdivided on the basis of the phenotypic classification by immunohistochemistry into steatotic, β -catenin, inflammatory, and unclassified subtypes (7,10). Immunohistochemical staining patterns and intensity of the HCAs relative to that of the adjacent liver parenchyma were compared. The expression of the transporter proteins was qualitatively assessed and compared with healthy liver by using a four-point scale: a grade of 0 indicated no expression; a grade of 1 indicated decreased expression relative to normal liver tissue; a grade of 2 indicated equivalent expression to normal liver tissue; and a grade of 3 indicated increased expression relative to adjacent liver. Grading was based on the area of the nodule with the highest degree of expression.

Statistical Analysis

The statistical analysis was performed by using commercially available software (MedCalc for Windows, version 9.3.2.0, MedCalc Software, Mariakerke, Belgium; and SPSS for Mac, version 21.0, SPSS, Chicago, Ill).

Descriptive statistics were calculated for clinical and imaging variables by using median and range for continuous variables, and frequencies and percentages for categorical variables. Because of the high interreader agreement, receiver operating characteristic curves were generated only for reader 1 to test the diagnostic performance of MR imaging features. The relationship between HBP appearance (ie, retention or washout), grade of transporter expression, and HCA subtype was assessed by using Spearman rank correlation coefficient and Pearson χ^2 test. Interreader agreement was calculated by using Cohen simple κ statistic

with 95% confidence intervals and was interpreted as follows: 0–0.20, slight agreement; 0.21–0.40, fair agreement; 0.41–0.60, moderate agreement; 0.61–0.80, substantial agreement; and 0.81–1.00, almost perfect agreement (30). *P* values less than .05 were indicative of statistical significance.

Results

Patient Characteristics

Twenty-nine patients with 43 histologic analysis–proven liver adenomas were included in this study. The majority of patients were women (23 of 29 patients [79%]) with a median age of 43 years (age range, 19–79 years). There were from one to 13 lesions per patient, with a medium tumor dimension of 38 mm (range, 5–125 mm). The histopathologic analysis after lesion biopsy (eight patients and eight lesions) or surgery (21 patients and 35 lesions) diagnosed 10 steatotic adenomas (25%), 21 inflammatory adenomas (49%), six β -catenin adenomas (13%), and six unclassified adenomas (13%). Sixteen of 29 patients (55%) had contributory clinical findings (Table 2; Table E2 [online]).

Imaging Characteristics and Enhancement Pattern

The lesion contour, signal intensity on T1- and T2-weighted images, and the presence of hepatic and lesion steatosis, pseudocapsule or atoll sign, central scar, hemorrhage, and/or necrosis and the dynamic enhancement pattern in the arterial, PV, and delayed postcontrast phases, and retention or washout of gadoteric acid in the HBP (Figs 2, 3) are tabulated for inflammatory, steatotic, β -catenin, and unclassified liver adenomas (Table 3).

Expression of Transporter Proteins

The OATP1B1/3 transporter had a decreased expression in nine of 10 steatotic and six of six unclassified lesions and an equivalent-to-increased expression in 16 of 21 inflammatory and five of six β -catenin lesions (*P* < .001) (Table E2 [online]). OATP1B1/3 expression was the main agent responsible for

Table 2

Demographics and Clinical Data

Parameter	Data
No. of patients	29
Total no. of lesions	43
No. of men	6 (21)
No. of women	23 (79)
Type of liver adenoma	
Steatotic	10 (23)
Inflammatory	21 (49)
β -catenin	6 (14)
Unclassified	6 (14)
No. of lesion biopsies	8 (19)
No. of surgeries	35 (81)
Clinical data of patients	
Metabolic syndrome	3 (10)
Obesity	6 (21)
Contraceptive or anabolic steroid use	4 (14)
Inflammatory syndrome	1 (3)
Glycogen storage disease	3 (10)
No underlying liver disease	12 (42)
Median continuous variables*	
Age at surgery or biopsy (y)	43 (19–79)
Men [†]	49 (21–59)
Women [†]	43 (19–79)
Max tumor dimension (mm)	38 (5–125)
No. of lesions	1 (1–13)

Note.—Data are numbers of patients or lesions unless otherwise indicated; data in parentheses are percentages unless otherwise indicated. There were 29 patients and 43 lesions.

* Data in parentheses are range.

[†] *P* = .6 according to Mann-Whitney test for continuous variables.

uptake of gadoteric acid in HCAs (*P* < .001) (Fig 4). OATP1B1/3 expression was significantly different between tumors that showed washout and those that showed retention on HBP images. All tumors with equivocal or increased expression of OATP1B1/3 showed contrast agent retention on HBP images (11 of 11 images [100%]), while tumors that showed decreased or no expression of OATP1B1/3 tended to show gadoteric acid washout on HBP images (21 of 32 images [66%]) (*P* < .001). There was a variable expression for MRP2 and MRP3 in the four types of liver adenomas (Table E2 [online]). Excretion was determined by MRP3 only (*P* = .003) (Fig 4); MRP2 appeared to

Figure 2

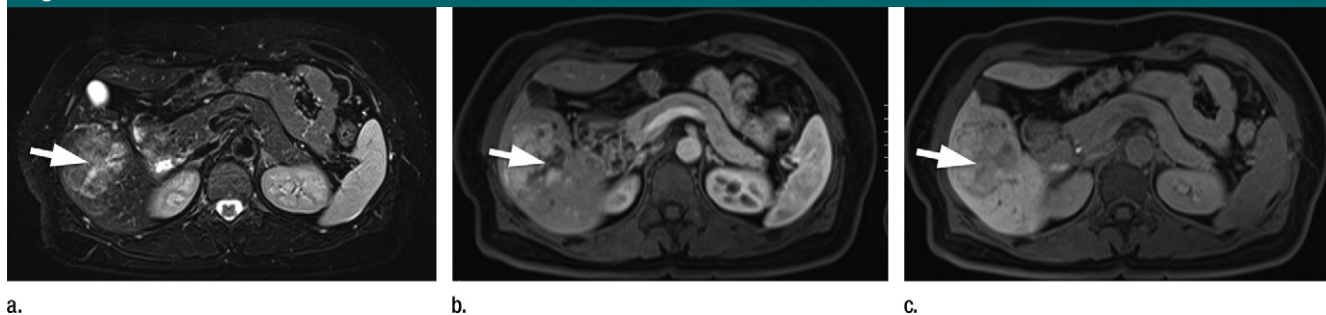


Figure 2: MR images in a 46-year-old woman with inflammatory syndrome (ie, fever, leukocytosis, and elevated C-reactive protein). A 5-cm mass in the right liver lobe is a moderately hyperintense lesion (arrow) with a peripheral prominent hyperintense band (the so-called atoll sign) on (a) axial T2-weighted image, (b) it strongly enhanced during the arterial phase of gadoteric acid–enhanced T1-weighted MR imaging, and (c) shows inhomogeneous contrast-agent retention during the HBP. Histologic analysis confirmed the diagnosis of inflammatory adenoma.

Figure 3

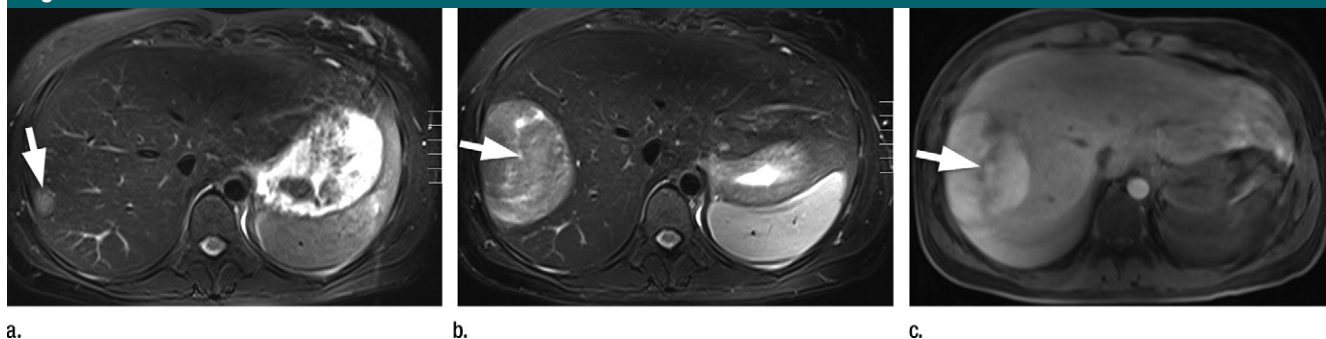


Figure 3: Images in a 24-year-old woman with metabolic syndrome. An encapsulated moderately hyperintense mass with a focal scar-like structure (arrow) on (a) axial T2-weighted baseline image and shows (b) dramatic increase on 2-year follow-up axial T2-weighted image and (c) inhomogeneous contrast-agent retention on gadoteric acid–enhanced T1-weighted MR image during the HBP. Histologic analysis confirmed a 10-cm adenoma that stained positive for β -catenin.

have no role ($P = .345$) (Fig 5). MRP3 expression was significantly different between the two tumor groups that showed washout and retention on HBP images (Table 4). More specifically, all tumors that showed no expression or decreased expression of MRP3 showed contrast agent retention on HBP images (11 of 11 images [100%]), while tumors that showed equivalent or increased expression of MRP3 tended to show contrast agent washout on HBP images (15 of 32 images [47%]) ($P = .008$) (Table 4).

Diagnostic Accuracy

The interreader agreement for the individual MR imaging features ranged from substantial to almost perfect ($\kappa = 0.72$ –1), whereas the κ value for the overall diagnostic performance was 0.85 (Table 5). Because of this excellent

agreement, the table lists the diagnostic findings of reader 1.

For the diagnosis of inflammatory adenoma, the area under the curve was 0.79 (95% confidence interval: 0.64, 0.90), sensitivity was 80.9% (17 of 21), specificity was 77.3% (17 of 22), positive predictive value was 77.3% (17 of 22), and negative predictive value was 81% (17 of 21); for the steatotic type, the area under the curve was 0.90 (95% confidence interval: 0.77, 0.97), sensitivity was 80% (eight of 10), specificity was 100% (33 of 33), positive predictive value was 100% (eight of eight), and negative predictive value was 94.3% (33 of 35); and for the β -catenin type, the area under the curve was 0.87 (95% confidence interval: 0.74, 0.95), sensitivity was 83.3% (five of six), specificity was 91.9% (34 of 37),

positive predictive value was 62.6% (five of eight), and negative predictive value was 97.1% (34 of 35). The area under the curve for the unclassified HCAs showed no statistical significance compared with chance (area under the curve, 0.62 [95% confidence interval: 0.46, 0.76]; sensitivity, 33.3% [two of six]; specificity, 91.9% [34 of 37]; positive predictive value, 40.1% [two of five]; negative predictive value, 89.4% [34 of 38]; $P = .33$).

Discussion

The results of this study suggest a mechanistic explanation for the retention and washout of gadoteric acid on HBP images of the HCA subtypes on the basis of the recent Bordeaux group classification (7,10). Our results, in which we used

gadoteric acid, corroborated those of previous studies; the majority, or 32 of 43 HCAs (75%), demonstrated washout in the HBP (13,14,31). However, in our cohort, 11 of 43 (25%) HCAs retained gadoteric acid and appeared inhomogeneously isointense to hyperintense on the HBP images. By analyzing our results in detail, we found that retention of gadoteric acid in the HBP was shown in six of 21 inflammatory adenomas, five of six β -catenin adenomas, but none of the 10 steatotic HCAs and none of the six unclassified HCAs. These results again are in accordance with recent reports in the literature (15–17). The retention of gadoteric acid in the HBP appears first quite logical because adenomas, like focal nodular hyperplasia, are considered as cholestatic lesions (ie, they have a limited ability to excrete this hepatobiliary contrast agent because of altered cell structure or blind-ending biliary ductules) (17,25). Even so, the majority of HCAs did show washout in the HBP, which suggests that hepatocellular uptake and excretion of gadoteric acid is not simply because of the abnormal anatomic connection to the biliary tree, and it may be more dependent on the expression of the hepatic transporters. By using semiquantitative immunohistochemistry, we set out to confirm this hypothesis (24). It is well known that gadoteric acid movement in hepatocytes is mediated by various transporters located on either the sinusoidal (OATP1B1/3 and MRP3) or canalicular (MRP2) membranes of the cell (19,22,32). Gadoteric acid enters the hepatocytes via active transport by OATP1B1/3 and is excreted into the biliary tree via MRP2 (23,28). Organic acid efflux from hepatocytes may also occur through the sinusoidal membrane because of bidirectional transport with OATP1B1/3 and MRP3 (23,28). We found that OATP1B1/3 expression was the main determinant responsible for uptake of gadoteric acid in HCAs ($P < .001$). Furthermore, excretion was determined by MRP3 only ($P = .003$). In general, the degree of OATP and MRP3 expression correlated with gadoteric acid retention and

Table 3

Imaging Features of Liver Adenoma Lesions for Reader 1

Imaging Variables	Inflammatory Lesions (n = 21)	Steatotic Lesions (n = 10)	Unclassified Lesions (n = 6)	β -Catenin Lesions (n = 6)
Opposed-phase T1 signal drop in nontumoral liver				
Absent	6 (24)	8 (80)	6 (100)	5 (83)
Present	15 (76)	2 (20)	0 (0)	1 (17)
Opposed-phase T1 signal loss in the lesion				
Absent	17 (81)	2 (20)	5 (83)	6 (100)
Mild	4 (19)	4 (40)	1 (17)	0 (0)
Severe	0 (0)	4 (40)	0 (0)	0 (0)
Diffuse	2 (9)	8 (80)	0 (0)	0 (0)
Focal	2 (9)	0 (0)	1 (17)	0 (0)
Contour				
Lobulated	15 (71)	5 (50)	3 (50)	6 (100)
Smooth	6 (29)	5 (50)	3 (50)	0 (0)
Atoll sign				
Absent	13 (62)	10 (100)	6 (100)	3 (50)
Present	8 (38)	0 (0)	0 (0)	3 (50)
Pseudocapsule				
Absent	8 (38)	8 (80)	3 (50)	3 (50)
Present	13 (62)	2 (20)	3 (50)	3 (50)
Central scar				
Absent	12 (57)	10 (100)	5 (83)	2 (33)
Present	9 (43)	0 (0)	1 (17)	4 (67)
Hemorrhage				
Absent	21 (100)	10 (100)	4 (67)	6 (100)
Present	0 (0)	0 (0)	2 (33)	0 (0)
Necrosis				
Absent	17 (81)	10 (100)	5 (83)	2 (33)
Present	4 (19)	0 (0)	1 (17)	4 (67)
T2-weighted SI				
Hypo/isointense	4 (19)	7 (70)	0 (0)	1 (17)
Moderately hyperintense	4 (19)	3 (30)	4 (67)	3 (50)
Strongly hyperintense	13 (62)	0 (0)	2 (33)	2 (33)
T1-weighted precontrast SI				
Hypointense	7 (34)	4 (40)	2 (33)	3 (50)
Isointense	11 (52)	2 (20)	3 (50)	3 (50)
Hyperintense	3 (14)	4 (40)	1 (17)	0 (0)
Postcontrast T1-weighted SI				
Arterial phase*				
Mild	0 (0)	1 (10)	0 (0)	0 (0)
Moderate	3 (14)	8 (80)	4 (67)	4 (67)
Severe	18 (86)	1 (10)	2 (33)	2 (33)
PV phase				
Washout	1 (5)	7 (70)	2 (33)	1 (17)
Persistence of contrast agent	20 (95)	3 (30)	4 (67)	5 (83)
Delayed phase 300 sec				
Washout	11 (52)	8 (80)	5 (83)	1 (17)
Persistence of contrast agent	10 (48)	2 (20)	1 (17)	5 (83)

Table 3 (continues)

Table 3 (continued)

Imaging Features of Liver Adenoma Lesions for Reader 1

Imaging Variables	Inflammatory Lesions (n = 21)	Steatotic Lesions (n = 10)	Unclassified Lesions (n = 6)	β -Catenin Lesions (n = 6)
HBP 20 min				
Washout	15 (71)	10 (100)	6 (100)	1 (17)
Retention	6 (29)	0 (0)	0 (0)	5 (83)

Note.—Data are number of lesions; data in parentheses are percentages. SI = signal intensity.

* The intensity of enhancement was defined as none, mild if less than PV, moderate if approximately equal to PV, or marked if approximately equal to aorta. Washout and retention is defined according to adjacent liver parenchyma.

Figure 4

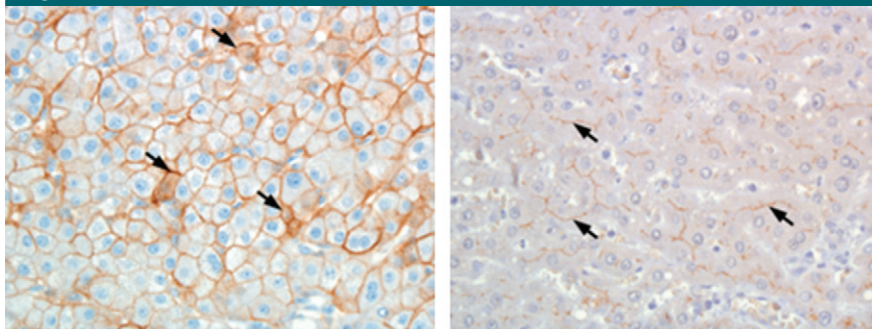


Figure 4: (a) Image shows immunohistochemistry with OATP1B1/3-specific stain. The brown cells indicate an overexpression of OATP1B/3 (OATP expression grade 3 [ie, increased expression relative to adjacent liver] adenoma; arrows) on the sinusoidal side in the inflammatory adenoma (shown in Fig 2) (original magnification, $\times 400$). (b) Image shows immunohistochemistry with MRP3-specific stain. The linear rust-colored bands demarcate areas of MRP3 overexpression (arrows) on the canalicular side in an inflammatory grade 3 adenoma (original magnification, $\times 400$).

washout, respectively. MRP2 appeared to have no significant role in the cholestatic feature of HCAs ($P = .345$).

Furthermore, our MR diagnostic accuracy is similar to those reported in previous publications (13–16,33); we found that the majority of steatotic and inflammatory HCAs demonstrated the classic morphologic features at T2 and precontrast T1 sequences and dynamic (ie, arterial and PV phases) enhancement pattern by using gadoxetic acid, which is similar to those reported that use gadolinium chelates (1,11,12). However, two steatotic HCAs showed no signal loss at opposed-phase sequences and were misclassified as inflammatory HCAs. Two inflammatory HCAs were classified correctly despite signal loss

at the opposed-phase sequence because the other features fit to this subtype. For the β -catenin type, we achieved very good sensitivity and specificity by using the presence of a central scar, hyperintense signal on T2-weighted images, and persistence of contrast on the PV and delayed phases (11,16).

Interestingly, most (five of six [83%]) β -catenin and 29% (six of 21) inflammatory HCAs mimicked focal nodular hyperplasia (ie, showed gadoxetic acid retention in HBP), which can pose a diagnostic dilemma (34). Whereas focal nodular hyperplasia requires neither follow-up nor treatment, inflammatory and β -catenin HCAs require intervention. Fortunately, 90% of focal nodular hyperplasia undergo

homogeneous gadoxetic retention in the HBP series in contrast to the heterogeneous retention pattern of inflammatory and β -catenin HCAs, which we found in our cohort as well (13,15,26). In addition, the higher T2-weighted signal intensity may favor the diagnosis of an adenoma (17,26). Furthermore, clinical risk factors can be useful to determine which of these lesions should, at least, be followed up (17). Eighty-five percent (17 of 20) of our patients with inflammatory and/or β -catenin HCA were obese or had metabolic syndrome, systemic inflammatory syndrome, and/or glycogen storage disease, and/or used oral contraceptives or steroids.

Although there are still no accepted guidelines for adenoma management, steatotic, unclassified, and inflammatory HCAs can be followed up if the lesions do not exceed 5 cm in diameter and do not grow (35). Surgical removal is indicated if any growth occurs (10). In the case of β -catenin HCAs, surgery is needed, independent of size (10,35).

Our study has several limitations. First, the total number of isointense or hyperintense HCAs on HBP examined was small because such tumors are relatively rare. However, we believe that the data obtained are sufficient to make some observations about the molecular biology of gadoxetic acid-enhanced MR imaging pharmacodynamics in the subtypes of HCAs. Rarer still are the β -catenin HCAs. Therefore, results that pertain to these lesions should be considered with caution.

Second, we showed that OATP1B1/3 and MRP3 expression correlated well with the enhancement patterns in the majority of HCAs. However, these results should be interpreted with caution because nonanionic and other organic cation transporters also participate in the uptake and washout of gadoxetic acid (32). As well, there may be genetic polymorphism among OATP transporters, which explains why there was a mismatch between transporter expression and the gadoxetic acid pattern in HBP in the remaining HCAs (19). Next, only part of our histopathologic specimens was en bloc resections. The remainder were biopsy specimens and

Figure 5

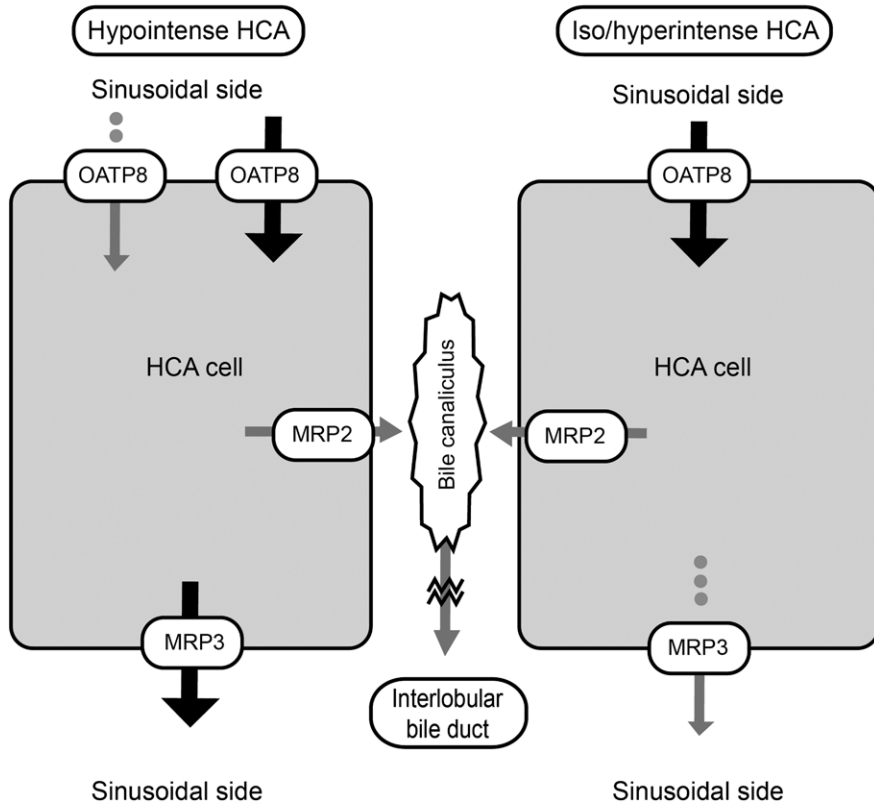


Figure 5: Diagram of the relationship between the OATP1B/3 and MRP3 regarding retention or washout of gadoxetic acid in the HBP. MRP2 appeared to have no substantial role, perhaps because of the absence of any connection to the bile ducts. The gray arrows indicate no function; the black arrows indicate full function. The wavy lines are no excretion because of the lack of connection to the bile ducts and the dots are absence of transporters.

Table 4

Correlations between Transporter Expression and Enhancement Pattern

Phase Type	OATP1B/3		MRP2		MRP3	
	Spearman Rank		Spearman Rank		Spearman Rank	
	Correlation Coefficient	P Value	Correlation Coefficient	P Value	Correlation Coefficient	P Value
Arterial phase enhancement	0.81	.2	0.004	.9	0.13	.3
PV phase	0.34	.02	-0.09	.5	-0.18	.2
Delayed phase 5 min	0.38	.01	-0.12	.4	-0.62	<.001
HBP 20 min	0.79	<.001	-0.13	.38	-0.57	<.001

Note.—The transporters only affected delayed and HBP phases. The degree of OATP and MRP3 expression correlated with gadoxetic acid retention and washout, respectively, in the HBP. MRP2 appeared to have no role.

thus subject to sampling error. Therefore, the degree of expression of transporter proteins might not have been correctly graded in biopsy specimens,

especially in heterogeneous lesions. One other limitation of this study is the overestimation of the diagnostic performance of gadoxetic acid–enhanced MR

Table 5

Interreader Agreement

Imaging Features	κ Value
Opposed-phase T1 signal loss	0.77
Lesion contour	0.84
Atoll sign	0.81
Pseudocapsule	0.91
Central scar	0.72
Hemorrhage	1
Necrosis	1
T2-weighted lesion signal intensity	0.86
T1-weighted lesion signal intensity	0.94
Arterial phase enhancement	0.96
PV phase, 70 sec	0.80
Delayed phase, 5 min	0.86
HBP, 20 min	0.94
Final radiologic diagnosis	0.85

Note.—Forty-three lesions were used for each parameter.

imaging in differentiating subtypes of HCAs because the readers were aware that the diagnosis must be some type of HCA. In clinical practice, we would have to differentiate not only from its HCA subtype, but also focal nodular hyperplasia or hepatocellular carcinoma in noncirrhotic livers. However, patient demographics (ie, age, sex, and clinical risk factors) favor one diagnosis over the others. Nevertheless, the near-perfect interobserver agreement confirms the ability of this technique to suggest the correct a priori classification of HCAs.

In conclusion, gadoxetic acid–enhanced MR imaging can favor the diagnosis of a specific type of HCA. Furthermore, the degree of OATP and MRP3 expression correlated with gadoxetic acid retention and washout, respectively, in the HBP. A prospective multicenter study is necessary to verify these promising results.

Disclosures of Conflicts of Interest: A.B.S. Activities related to the present article: disclosed no relevant relationships. Activities not related to the present article: author received honoraria for lectures from Bayer Health Care. Other relationships: disclosed no relevant relationships. C.A. disclosed no relevant relationships. D.F. disclosed no relevant relationships. N.B. disclosed no relevant relationships. J.C.H. disclosed no relevant relationships. J.S. disclosed no relevant relationships. M.A.C. disclosed no

relevant relationships. **F.W.** disclosed no relevant relationships. **M.T.** disclosed no relevant relationships. **C.J.H.** disclosed no relevant relationships. **F.C.A.** disclosed no relevant relationships.

References

- Ronot M, Bahrami S, Calderaro J, et al. Hepatocellular adenomas: accuracy of magnetic resonance imaging and liver biopsy in subtype classification. *Hepatology* 2011;53(4):1182–1191.
- Grazioli L, Olivetti L, Mazza G, Bondioni MP. MR imaging of hepatocellular adenomas and differential diagnosis dilemma. *Int J Hepatol* 2013;2013:374170.
- Shanbhogue AK, Prasad SR, Takahashi N, Vikram R, Sahani DV. Recent advances in cytogenetics and molecular biology of adult hepatocellular tumors: implications for imaging and management. *Radiology* 2011;258(3):673–693.
- Katabathina VS, Menias CO, Shanbhogue AK, Jagirdar J, Paspulati RM, Prasad SR. Genetics and imaging of hepatocellular adenomas: 2011 update. *RadioGraphics* 2011;31(6):1529–1543.
- Bioulac-Sage P, Sempoux C, Possenti L, et al. Pathological diagnosis of hepatocellular adenoma according to the clinical context. *Int J Hepatol* 2013;2013:253261.
- Sempoux C, Chang C, Gouw A, et al. Benign hepatocellular nodules: what have we learned using the patho-molecular classification. *Clin Res Hepatol Gastroenterol* 2013;37(4):322–327.
- Zucman-Rossi J, Jeannot E, Nhieu JT, et al. Genotype-phenotype correlation in hepatocellular adenoma: new classification and relationship with HCC. *Hepatology* 2006;43(3):515–524.
- Dokmak S, Paradis V, Vilgrain V, et al. A single-center surgical experience of 122 patients with single and multiple hepatocellular adenomas. *Gastroenterology* 2009;137(5):1698–1705.
- Farges O, Dokmak S. Malignant transformation of liver adenoma: an analysis of the literature. *Dig Surg* 2010;27(1):32–38.
- Bioulac-Sage P, Laumonier H, Couchy G, et al. Hepatocellular adenoma management and phenotypic classification: the Bordeaux experience. *Hepatology* 2009;50(2):481–489.
- van Aalten SM, Thomeer MG, Terkivatan T, et al. Hepatocellular adenomas: correlation of MR imaging findings with pathologic subtype classification. *Radiology* 2011;261(1):172–181.
- Laumonier H, Bioulac-Sage P, Laurent C, Zucman-Rossi J, Balabaud C, Trillaud H. Hepatocellular adenomas: magnetic resonance imaging features as a function of molecular pathological classification. *Hepatology* 2008;48(3):808–818.
- Grazioli L, Bondioni MP, Haradome H, et al. Hepatocellular adenoma and focal nodular hyperplasia: value of gadoteric acid-enhanced MR imaging in differential diagnosis. *Radiology* 2012;262(2):520–529.
- Giovanoli O, Heim M, Terracciano L, Bongartz G, Ledermann HP. MRI of hepatic adenomatosis: initial observations with gadoteric acid contrast agent in three patients. *AJR Am J Roentgenol* 2008;190(5):W290–W293.
- Thomeer MG, Willemsen FE, Biermann KK, et al. MRI features of inflammatory hepatocellular adenomas on hepatocyte phase imaging with liver-specific contrast agents. *J Magn Reson Imaging* 2014;39(5):1259–1264.
- Yoneda N, Matsui O, Kitao A, et al. Beta-catenin-activated hepatocellular adenoma showing hyperintensity on hepatobiliary-phase gadoteric acid-enhanced magnetic resonance imaging and overexpression of OATP8. *Jpn J Radiol* 2012;30(9):777–782.
- Agarwal S, Fuentes-Orrego JM, Arnason T, et al. Inflammatory hepatocellular adenomas can mimic focal nodular hyperplasia on gadoteric acid-enhanced MRI. *AJR Am J Roentgenol* 2014;203(4):W408–W414.
- Denecke T, Steffen IG, Agarwal S, et al. Appearance of hepatocellular adenomas on gadoteric acid-enhanced MRI. *Eur Radiol* 2012;22(8):1769–1775.
- Nassif A, Jia J, Keiser M, et al. Visualization of hepatic uptake transporter function in healthy subjects by using gadoteric acid-enhanced MR imaging. *Radiology* 2012;264(3):741–750.
- Hagenbuch B, Meier PJ. Organic anion transporting polypeptides of the OATP/SLC21 family: phylogenetic classification as OATP/SLCO superfamily, new nomenclature and molecular/functional properties. *Pflugers Arch* 2004;447(5):653–665.
- Narita M, Hatano E, Arizono S, et al. Expression of OATP1B3 determines uptake of Gd-EOB-DTPA in hepatocellular carcinoma. *J Gastroenterol* 2009;44(7):793–798.
- Kitao A, Matsui O, Yoneda N, et al. The uptake transporter OATP8 expression decreases during multistep hepatocarcinogenesis: correlation with gadoteric acid enhanced MR imaging. *Eur Radiol* 2011;21(10):2056–2066.
- Kitao A, Zen Y, Matsui O, et al. Hepatocellular carcinoma: signal intensity at gadoteric acid-enhanced MR imaging—correlation with molecular transporters and histopathologic features. *Radiology* 2010;256(3):817–826.
- Vander Borgh S, Libbrecht L, Blokzijl H, et al. Diagnostic and pathogenetic implications of the expression of hepatic transporters in focal lesions occurring in normal liver. *J Pathol* 2005;207(4):471–482.
- Grazioli L, Morana G, Kirchin MA, Schneider G. Accurate differentiation of focal nodular hyperplasia from hepatic adenoma at gadobenate dimeglumine-enhanced MR imaging: prospective study. *Radiology* 2005;236(1):166–177.
- Grieser C, Steffen IG, Seehofer D, et al. Histopathologically confirmed focal nodular hyperplasia of the liver: gadoteric acid-enhanced MRI characteristics. *Magn Reson Imaging* 2013;31(5):755–760.
- International Working Party. Terminology of nodular hepatocellular lesions. *Hepatology* 1995;22(3):983–993.
- Halilbasic E, Claudel T, Trauner M. Bile acid transporters and regulatory nuclear receptors in the liver and beyond. *J Hepatol* 2013;58(1):155–168.
- Lee TC, Ho IC, Lu WJ, Huang JD. Enhanced expression of multidrug resistance-associated protein 2 and reduced expression of aquaglyceroporin 3 in an arsenic-resistant human cell line. *J Biol Chem* 2006;281(27):18401–18407.
- Altman DG. *Practical statistics for medical research*. Boca Raton, Fla.: Chapman & Hall/CRC, 1999.
- Ringe KI, Husarik DB, Sirlin CB, Merkle EM. Gadoteric disodium-enhanced MRI of the liver: part 1, protocol optimization and lesion appearance in the noncirrhotic liver. *AJR Am J Roentgenol* 2010;195(1):13–28.
- Leonhardt M, Keiser M, Oswald S, et al. Hepatic uptake of the magnetic resonance imaging contrast agent Gd-EOB-DTPA: role of human organic anion transporters. *Drug Metab Dispos* 2010;38(7):1024–1028.
- Manichon AF, Bancel B, Durieux-Millon M, et al. Hepatocellular adenoma: evaluation with contrast-enhanced ultrasound and MRI and correlation with pathologic and phenotypic classification in 26 lesions. *HPB Surg* 2012;2012:418745.
- Paradis V, Champault A, Ronot M, et al. Telangiectatic adenoma: an entity associated with increased body mass index and inflammation. *Hepatology* 2007;46(1):140–146.
- Blanc JF, Frulio N, Chiche L, et al. Hepatocellular adenoma management: Call for shared guidelines and multidisciplinary approach. *Clin Res Hepatol Gastroenterol* 2014.